

## Design of a Sliding Mode Controller for a Solar Boost Inverter

S.Sivaranjani<sup>1</sup> Dr.A.Ezhilarasi<sup>2</sup> Dr M.Ramaswamy<sup>3</sup>

<sup>1</sup>(Research Scholar, Dept of Electrical Engineering, Annamalai University Nagar-608 002, Tamil Nadu, India)

<sup>2</sup>(Assistant Professor, Dept of Electrical Engineering, Annamalai University Nagar-608 002, Tamil Nadu, India)

<sup>3</sup>(Professor, Dept of Electrical Engineering, Annamalai University Nagar-608 002, Tamil Nadu, India)

Corresponding Author: S.Sivaranjani

**Abstract:** The paper attempts to design a sliding mode controller (SMC) for a solar boost inverter with a view to regulate the output voltage and reduce its total harmonic distortion (THD) over a range of operating loads. The philosophy of the inverter relates to extracting an ac output at the desired amplitude and frequency from the available solar power input. The ability of the chosen topology to offer a sinusoidal voltage gathers interest in the perspective of allowing the output to be interfaced with the grid. The theory of the control strategy encompasses measures to increase the fundamental component and lower the higher frequency components of the output voltage. The simulation results bring out the relative merits of SMC over the conventional PI controller in terms of a lower THD for the output voltage. The experimental results forge to validate the simulated performance and espouse the inverter along with the SMC to claim a place for its use both in real world and grid connected utilities.

**Keywords:** Solar boost inverter, sliding mode control(SMC),voltage regulation, total harmonic distortion(THD).

Date of Submission: 14-12-2018

Date of acceptance: 29-12-2018

### I. INTRODUCTION

The power converters enjoy a role in various applications in the sense it converts the available form of energy to the desired form. The advantage of the power semiconductor devices like case of control, increased power capability and the reduced cost enable the converters to become affordable, the inverter forms a power electronic converter where the dc power can be converted into the ac power at the desired rms value and frequency [1]. The boost inverter exhibits several advantages, the most important of which owe to the fact that it can generate an ac output voltage from a lower dc input voltage in a single power stage using MOSFET switches.

The main attribute of the boost inverter topology engages the cause that it generates an ac output voltage larger than that dc input, depending on the instantaneous duty cycle. It finds its use in UPS, electric motor speed control, refrigeration compressors, power grid, induction heating and HVDC power transmission systems [2]. The shoot through state, where both the power switches in a leg if turned on at the same time characterizes to be forbidden in the dc- ac inverter, because it constitutes a short circuit across the capacitor and damage the devices. A dead time can be inserted into the upper and lower switches in a leg to operate against the short circuit, while increasing the output waveform distortion.

The single stage non isolated inverter topologies has been seen to be attractive because of the reduced number of components and in light of the fact that the power stage accrues a lower cost and offers a more efficient conversion, unless the inverter requires isolation between the input/output [3].A two stage operation with a dc-dc boost and a dc-ac buck stages, widely used in practice has been found to suffer from lower efficiency and higher cost due to the two stages [4].

A single stage boost inverter composed of two individual boost converters has been suggested due to its simple structure and ease of operation [5]. The boost converter has been driven by two phase shift dc-bias sinusoidal references and the differential output forms the ac utility line voltage. The grid connected current controlled boost inverter has been introduced to minimize the problems with a two stage fuel cell power conditioning system and evolve a topology suitable for ac loads, with reduced power processing and conversion stages [6]. A one cycle control (OCC) has been applied to a single stage grid connected inverter and seen to be reliable, universal and fast. Besides a hybrid control scheme with adaptive neuro fuzzy inference system (ANFIS) has been showcased to obtain a high voltage gain and a low THD for the single stage boost inverter [7]. The boost inverter in [8], has been differentially connected between the outputs of two bidirectional boost converters to provide a true sinusoidal output.

A double-loop control scheme with an inductor current control inner loop and an output voltage control outer loop has been developed to govern the operation of a boost inverter [9]. Both the control loops have been based on the averaged continuous-time model of the boost topology and a feed forward control technique proposed to improve the system robustness against external disturbances. Despite the aforesaid developments there exists an urge to explore new control approaches owing to numerous challenges that invite attention from the utility sector [10].

## II. PROBLEM FORMULATION

The primary objective echoes to design a sliding mode controller (SMC) for regulating the output voltage and reducing its total harmonic distortion (THD) for a solar boost inverter, across its operating range. The scope extends to explore the use of an Atmel processor for generating the PWM pulses for the power switches. The effort relates to validating the simulation results through the use of a prototype and establishing its supremacy over that of a PI controller.

## III. PROPOSED STRATEGY

The theory relies on the use of the SMC with the pulse width modulation (PWM) strategy for reducing the THD of the output voltage and ensuring a better quality of transfer the power to the load.

### 3.1 POWER MODULE

The boost inverter consists of two bidirectional boost converter with their outputs connected in series as shown in Fig. 1. Each boost converter generates a dc bias with deliberate ac output voltage so that the output of each converter offers a unipolar voltage, greater than the input voltage and allows to be operated with a variable duty cycle.

The dc - ac boost inverter can be explained by considering the two modes of operation with  $V_{in}$  being the input dc voltage and connected with the two inductance  $L_1$  and  $L_2$ ,  $S_1, S_2, S_3$  and  $S_4$  to be the series semiconductor switches, The capacitor  $C_1$  and  $C_2$  remain connected across each boost converter, whose output voltage creates 180 degree out of phase with each other, R is the load resistance respectively.

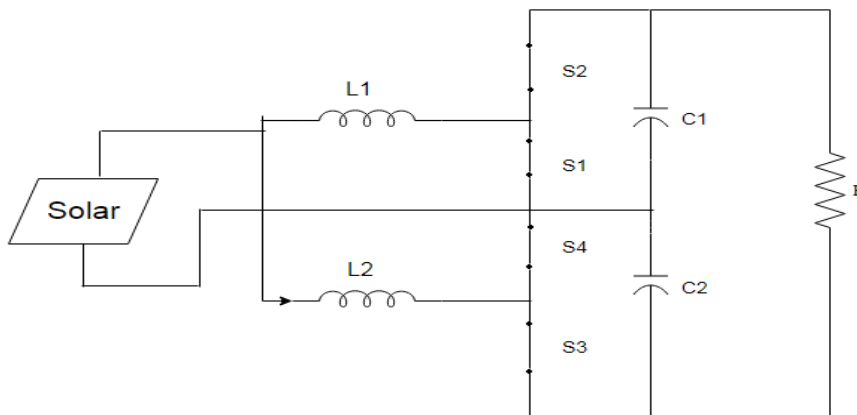


Fig. 1 Structure of Boost Inverter

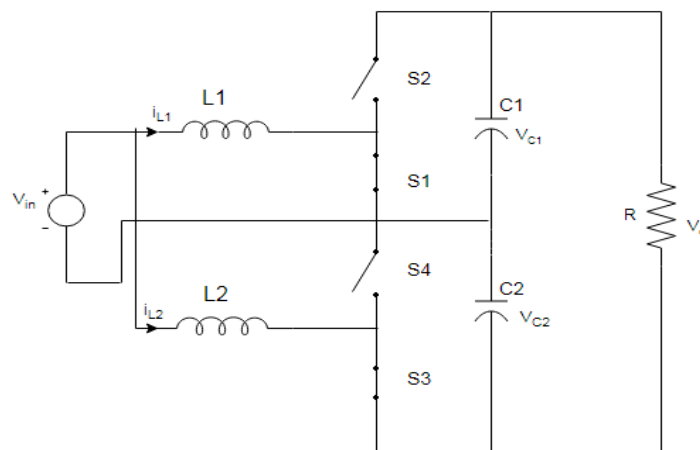


Fig. 2 Circuit diagram of boost inverter for Mode 1 operation

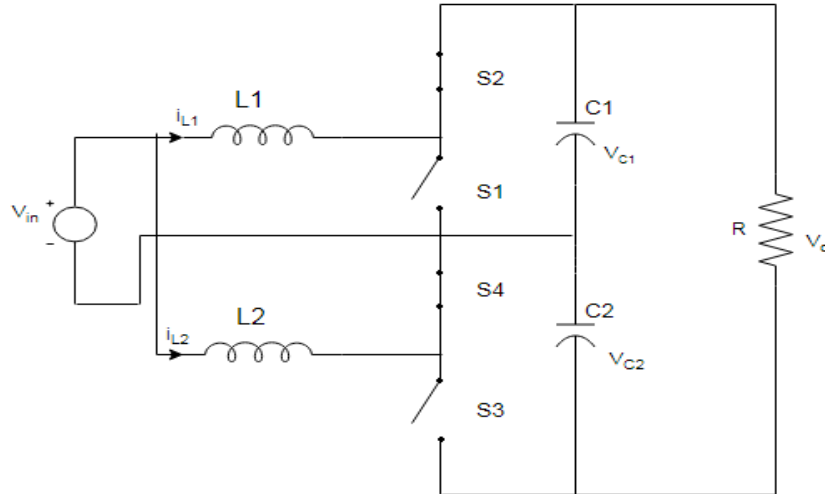


Fig. 3 Circuit diagram of boost inverter for Mode 2 operation

### 3.2 MODELING

The model plays a significant role in the development of complex system on account of the fact they facilitate a better understanding of the variables and the parameters affecting the system performance. Besides it serves as a tool to include new devices and predict its behavior almost instantaneously. The modeling and analysis of switching dc-ac converters can be either numerical or analytical. There exists a host of algorithms or circuit dc-ac simulators to produce quantitative results in numerical approaches.

It models the system in the differential domain where the inverter can be controlled to deliver active power to the load, keeping the output voltage constant. By applying KVL and KCL to the different switching states of the simplified circuit, the system can be modeled for the differential mode of operation with the current flow for the positive half cycle and negative half cycle seen in Fig. 2 and 3 respectively. The state space model of series connected boost inverter can be described as follows

Mode 1:

With the switches S<sub>1</sub> and S<sub>3</sub> turned on, the switches S<sub>2</sub> and S<sub>4</sub> turned off. While the inductor L<sub>1</sub> charges the inductor L<sub>2</sub> discharges and the capacitor C<sub>2</sub> charges through the inductor L<sub>2</sub>. The capacitor C<sub>1</sub> discharges to support the load resistor R.

The Eqns. [1] through [4] obtained by applying Kirchhoff's law for the inverter circuit in Fig. 2 reflect the operation in Mode 1

$$\frac{di_{L1}}{dt} = \frac{V_{in}}{L_1} \quad \text{----- (1)}$$

$$\frac{dV_{C1}}{dt} = -\frac{V_0}{RC_1} \quad \text{----- (2)}$$

$$\frac{di_{L2}}{dt} = \frac{v_{in}}{L_2} - \frac{V_{C2}}{L_2} \quad \text{----- (3)}$$

$$\frac{dV_{C2}}{dt} = \frac{i_{L2}}{C_2} - \frac{V_{C2}}{RC_2} \quad \text{----- (4)}$$

The Eqn. (5) gives the general state space equation

$$\dot{X} = AX + BU \quad \text{----- (5)}$$

Using the state space equation, the state matrix can be written as follows

$$\begin{bmatrix} \frac{di_{L1}}{dt} \\ \frac{dV_{C1}}{dt} \end{bmatrix} = \begin{bmatrix} 0 & 0 \\ 0 & -\frac{1}{RC_1} \end{bmatrix} \begin{bmatrix} i_{L1} \\ v_{C1} \end{bmatrix} + \begin{bmatrix} \frac{1}{L_1} \\ 0 \end{bmatrix} V_{in} \quad \text{----- (6)}$$

$$\begin{bmatrix} \frac{di_{L2}}{dt} \\ \frac{dV_{C2}}{dt} \end{bmatrix} = \begin{bmatrix} 0 & -1 \\ \frac{1}{C_2} & \frac{-1}{RC_2} \end{bmatrix} \begin{bmatrix} i_{L2} \\ v_{C2} \end{bmatrix} + \begin{bmatrix} \frac{1}{L_2} \\ 0 \end{bmatrix} V_{in} \text{ ----- (7)}$$

Mode 2:

Similarly with the switches  $S_2$  and  $S_4$  turned on, the switches  $S_1$  and  $S_3$  turned off, while the inductor  $L_2$  charges, the inductor  $L_1$  discharges and the capacitor  $C_1$  charges. The capacitor  $C_2$  discharges and delivers power to the load resistor  $R$ .

The Eqns. (8) through (11) can be obtained by applying Kirchoff's law to the inverter circuit in Fig 3 and explains the operation of the circuit in the second mode

$$\frac{di_{L1}}{dt} = \frac{v_{in}}{L_1} - \frac{V_{C1}}{L_1} \text{ ----- (8)}$$

$$\frac{dV_{C1}}{dt} = \frac{i_{L1}}{C_1} - \frac{V_{C1}}{RC_1} \text{ ----- (9)}$$

$$\frac{di_{L2}}{dt} = \frac{V_{in}}{L_2} \text{ ----- (10)}$$

$$\frac{dV_{C2}}{dt} = -\frac{V_{C2}}{RC_2} \text{ ----- (11)}$$

The Eqns. (12) and (13) give the corresponding state space equations of Mode 2

$$\begin{bmatrix} \frac{di_{L1}}{dt} \\ \frac{dV_{C1}}{dt} \end{bmatrix} = \begin{bmatrix} 0 & -1 \\ \frac{1}{C_1} & \frac{-1}{RC_1} \end{bmatrix} \begin{bmatrix} i_{L1} \\ v_{C1} \end{bmatrix} + \begin{bmatrix} \frac{1}{L_1} \\ 0 \end{bmatrix} V_{in} \text{ ----- (12)}$$

$$\begin{bmatrix} \frac{di_{L2}}{dt} \\ \frac{dV_{C2}}{dt} \end{bmatrix} = \begin{bmatrix} 0 & 0 \\ 0 & \frac{-1}{RC_2} \end{bmatrix} \begin{bmatrix} i_{L2} \\ v_{C2} \end{bmatrix} + \begin{bmatrix} \frac{1}{L_2} \\ 0 \end{bmatrix} V_{in} \text{ ----- (13)}$$

Invoking the state space averaging technique in Eqn. (14)

$$\begin{aligned} A &= A_1(D) + A_2(1 - D) \\ B &= B_1(D) + B_2(1 - D) \text{ ----- (14)} \end{aligned}$$

The Eqn. (15) and (16) are obtained by using state space average technique

$$\begin{bmatrix} \frac{di_{L1}}{dt} \\ \frac{dV_{C1}}{dt} \end{bmatrix} = \begin{bmatrix} 0 & \frac{-(1-D)}{L_1} \\ \frac{(1-D)}{C_1} & \frac{-1}{RC_1} \end{bmatrix} \begin{bmatrix} i_{L1} \\ v_{C1} \end{bmatrix} + \begin{bmatrix} \frac{1}{L_1} \\ 0 \end{bmatrix} V_{in} \text{ ----- (15)}$$

$$\begin{bmatrix} \frac{di_{L2}}{dt} \\ \frac{dV_{C2}}{dt} \end{bmatrix} = \begin{bmatrix} 0 & \frac{-(1-D)}{L_2} \\ \frac{(1-D)}{C_2} & \frac{-1}{RC_2} \end{bmatrix} \begin{bmatrix} i_{L2} \\ v_{C2} \end{bmatrix} + \begin{bmatrix} \frac{1}{L_2} \\ 0 \end{bmatrix} V_{in} \text{ ----- (16)}$$

It follows that  $V_o = V_{C1} - V_{C2}$

$$\frac{dV_o}{dt} = \frac{dV_{C1}}{dt} - \frac{dV_{C2}}{dt} \text{ ----- (17)}$$

The Eqn. (15) and (16) combine to form the final matrix of the boost inverter in Eqn. (18)

$$\begin{bmatrix} \frac{di_{L1}}{dt} \\ \frac{di_{L2}}{dt} \\ \frac{dV_o}{dt} \end{bmatrix} = \begin{bmatrix} 0 & 0 & \frac{-(1-D)}{L_1} \\ 0 & 0 & \frac{-(1-D)}{L_2} \\ \frac{(1-D)}{C_1} & \frac{-(1-D)}{C_2} & \frac{-1}{RC_1} \end{bmatrix} \begin{bmatrix} i_{L1} \\ i_{L2} \\ V_o \end{bmatrix} + \begin{bmatrix} \frac{1}{L_1} \\ \frac{1}{L_2} \\ 0 \end{bmatrix} V_{in} \text{ ----- (18)}$$

The philosophy of the controller can be deduced from the state space equivalent circuits and therefore the sliding mode equation derived through the expression  $s(x) = 0$ .

#### IV. CONTROL ALGORITHM

A control technique suitable for dc-ac converter must cope with their intrinsic nonlinearity and wide input voltage and load variations to ensure stability in any operating condition while providing fast transient response. The dc-ac energy conversion includes both the boost and inversion stages and provides high power conversion efficiency, reduced converter size and low cost .It operates using the double-loop control scheme for it being the most appropriate method to control the individual boost converter across the wide range of operating points [11]. Using this control method, the inverter maintains a stable operating condition by means of limiting the inductor current.

The Fig 4 represents the basic circuit diagram of the boost inverter with the introduction of the SMC. It begins with the selection of sliding surface [12] and the continuous increase in current allows the direct surface  $V_0 - V_{ref}$  nearly to zero [13] through the use of two cascaded control loops. The voltage error from the outer voltage loop produces the reference current. The stability criteria and existence of sliding mode can be achieved by controlling the output voltage of ac-dc inverter. The inductor current can be controlled by the inner current loop through sliding mode technique. The voltage loop being highly sensitive to the high frequency switching and the uncertainties in the reference current necessitates SMC to track and enable the regulation of the output voltage [14].

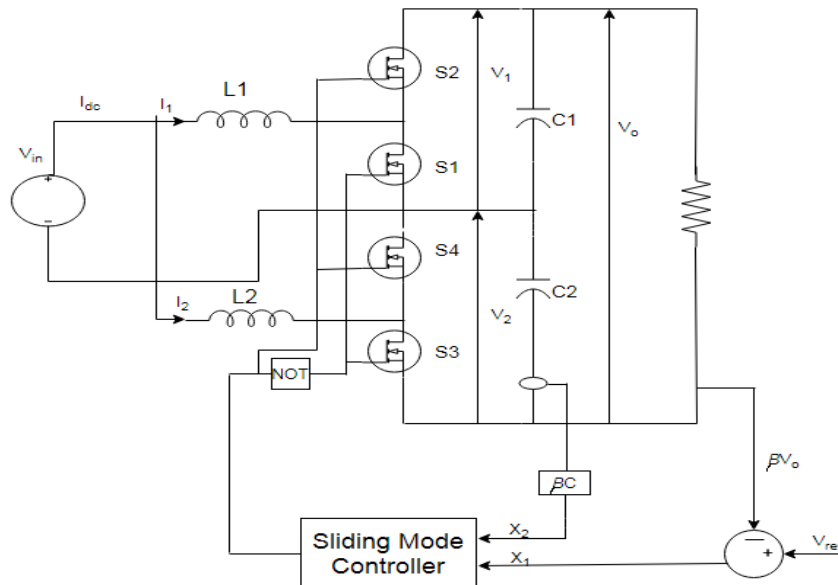


**Fig. 4** Boost inverter with SMC

The Eqn. (19) represent the voltage error,  $X_1$

$$X_1 = V_{ref} - \beta V_o \text{ ----- (19)}$$

Where  $V_{ref}$  refers to the constant reference voltage and  $\beta$  the sensing ratio of the output voltage. The rate of change of voltage error,  $X_2$  maybe expressed as in Eqn. 20

$$X_2 = \dot{X}_1 = -\beta \frac{dV_o}{dt} = \beta \frac{I_c}{C} \text{ ----- (20)}$$

Where  $I_c = C(dV_o/dt)$  gives the capacitor current, and  $C$  is the capacitance. Since  $I_c = I_L - I_R$  where  $I_L$  and  $I_R$  represent the inductor and load currents respectively, the differentiation of the above equation with respect to the time gives Eqn. 21

$$\dot{X}_2 = \frac{\beta}{C} \frac{d(I_R - I_L)}{dt} \text{ ----- (21)}$$

Using  $I_R = V_o/R_L$  Where  $R_L$  refers the load resistance, and the averaged equation of a inductor current, the inductor can be written as in Eqn. 22

$$I_L = \int \frac{uV_i - V_o}{L} dt \text{ ----- (22)}$$

Where  $V_i$  relates to the input voltage,  $L$  the inductance, and  $u = 1$  or  $0$  the switching state. It rearranges as in Eqn. 23

$$\dot{X}_2 = \frac{\beta}{R_L C} - \frac{dV_o}{dt} + \frac{\beta(V_o - uV_i)}{L} = -\frac{X_2}{R_L C} + \frac{V_{ref}}{LC} - \frac{X_1}{LC} - u \frac{\beta V_i}{LC} \text{ ----- (23)}$$

The state space model describing the system can be derived as in Eqn. 24

$$\begin{bmatrix} \dot{X}_1 \\ \dot{X}_2 \end{bmatrix} = \begin{bmatrix} 0 & 1 \\ -\frac{1}{LC} & -\frac{1}{R_L C} \end{bmatrix} \begin{bmatrix} X_1 \\ X_2 \end{bmatrix} + \begin{bmatrix} 0 \\ -\beta V_i / LC \end{bmatrix} u + \begin{bmatrix} 0 \\ \frac{V_{ref}}{LC} \end{bmatrix} \text{ ----- (24)}$$

The sliding line in Eqn.25 decides the switching states  $u$ , which corresponds the turning on and off of the power converter switch

$$S = \alpha X_1 + X_2 = JX = 0 \text{ ----- (25)}$$

Where  $\alpha$  becomes a positive quantity (stability condition), loss function  $J = [\alpha, 1]$ ,  $X = [X_1 \ X_2]^T$ . It can thus be derived as in Eqn. 26

$$\alpha = \frac{1}{R_L C} \text{ ----- (26)}$$

The switching conditions necessitates to an existing condition and the Eqn.27 can be obtained by the Eqn.19 and 20

$$S = K_1 (V_{ref} - \beta V_o) + K_2 i_c \text{ ----- (27)}$$

Where  $K_1 = \frac{1}{R_L C}$      $K_2 = \frac{\beta}{C}$

$$S = \left(\frac{1}{\beta} R_L\right) (V_{ref} - \beta V_o) - i_c \text{ ----- (28)}$$

If the sliding condition exists, then the system trajectory shall move along the designed sliding surface, so long as the above conditions remain satisfied.

## V. SIMULATION RESULTS

The exercise owes to evaluate the performance of the single stage dc-ac boost inverter using MATLAB based simulation. The elements of the inverter under study relate to inductance  $L_1$  &  $L_2 = 5\text{mH}$ , capacitance  $C_1$  &  $C_2 = 90\mu\text{F}$ , switching frequency  $F_s = 50\text{ kHz}$  and the load resistance allowed to varied up to  $5\text{KW}$ . The system acquires the input from series connected solar panels with the specifications in Table 1 to offer the input voltage of  $70\text{V}$  and attempts to provide an ac output voltage of  $120\text{V}$ .

**Table 1** Solar specification

<b>PV Module</b>	
Number of cells in module	36
Open circuit voltage	21 V
Short circuit current	6.4 A
Voltage at MPP, $V_m$	17 V
Current at MPP, $I_m$	5.4 A

PV Array	
Voltage at MPP, $V_{mpp} = V_{pv}$	140
Power at $M_{pp}$ , $P_{mpp} = P_{pv}$	2000W
Current at $M_{pp}$ ,	13.3 A
No. of series Modules $N_s$	$V_{mpp} / V_m = 9$
No. of parallel Modules $N_p$	$I_{mpp} / I_m = 2$

The Figs. 5 and 6 depict the output voltage of the inverter and the load current corresponding to a load power of 1.5KW using PI and SMC controller. The regulating phenomena of the output voltage in the event of sudden changes in supply and load introduced at 0.3 sec and 1 sec respectively. The SMC encompasses with it the mechanism to choose the appropriate value of the duty cycle to restore the desired load voltage. The THD spectrum displayed in Fig 7 and 8 drawn for the same operating point enumerates the ability of the SMC to pull out a lower THD for the output voltage of the inverter over the PI controller

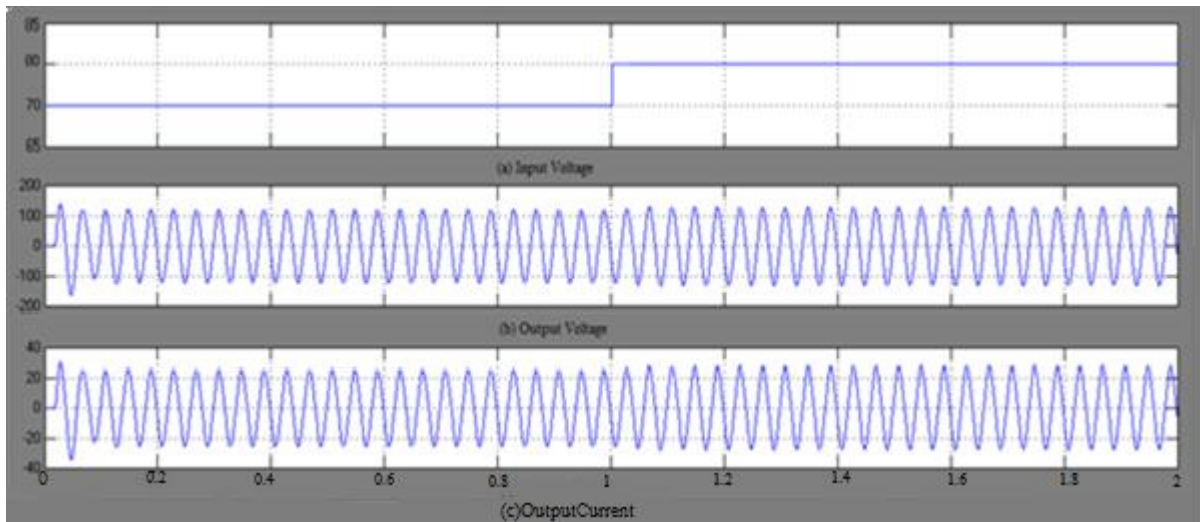


Fig. 5 Steady state transient wave form for PI

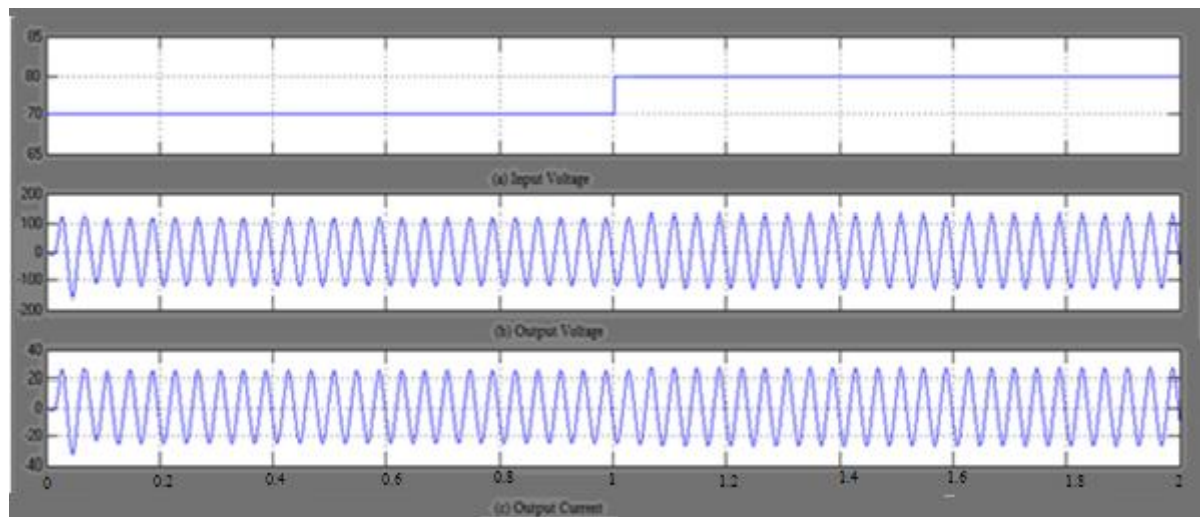


Fig. 6 Steady state transient waveform for SMC

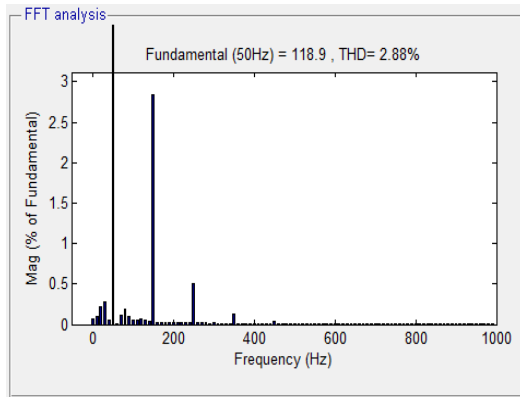


Fig. 7 THD in SMC

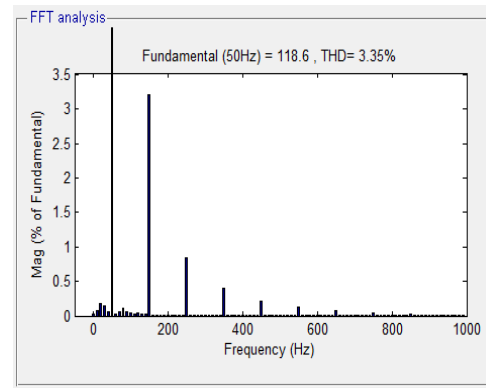


Fig. 8 THD in PI

### VI. HARDWARE IMPEMENTATION

The experimental setup shown in fig. 9 consists of the input from solar PV module and the dc-ac inverter along with the resistive load. It owes to examine the performance of the methodology over similar ratings as that used in simulation through the operating range. The control circuit operates from the available ac supply through a step-down transformer (230/15) V, a diode bridge rectifier, an integrator circuit and a capacitor filter to remove the ripples. The system involves the use of an Atmel processor for generating the pulses for the IGBT switches in tune with the design of the control strategy. The flow chart in Fig. 10 explains the steps involved in programming the processor for reaching out to acquiring the pulses



Fig.9 Prototype



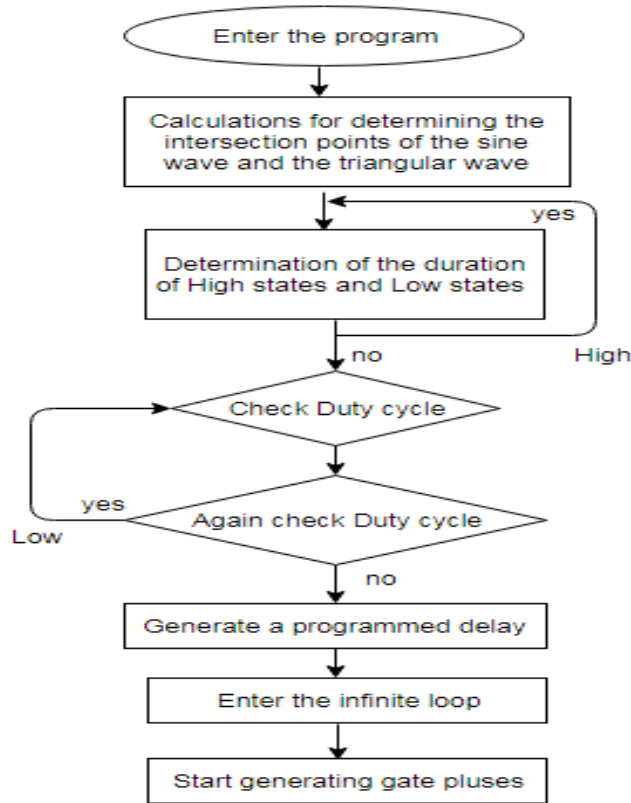


Fig 10 Flow Chart

The Figs. 11, 12, 13, and 14 displays the output voltage, output voltage THD, output current and output current THD, corresponding to the same operating point. The sinusoidal nature of the voltage reflects the benefits of the inverter and the efficacy of the control algorithm.

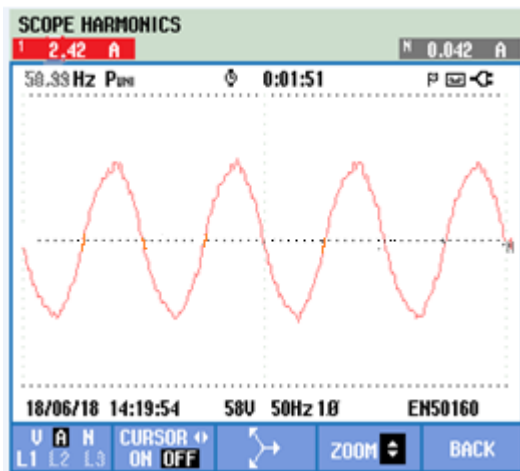


Fig 11 Output current

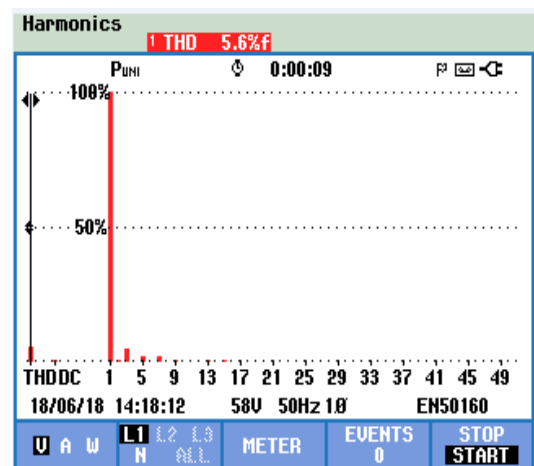


Fig 12 Output voltage THD

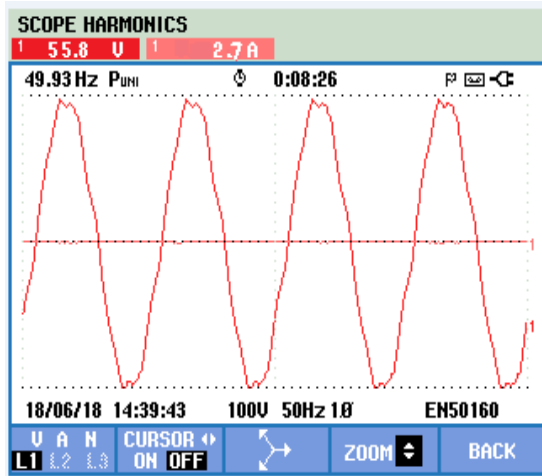


Fig 13 Output voltage

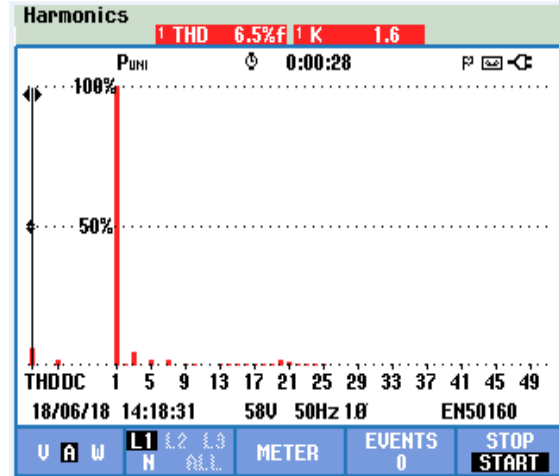


Fig 14 Output current THD

The entries in Table.2 compare the values of the load current, load voltage and its THD for various values of load power, obtained using SMC with that of the PI in an attempt to validate the methodology and establish the supremacy of the SMC. It follows that the output voltage remains regulated through the operating range and the philosophy extricates a lower THD for the load voltage.

Table: 2 Performance Comparisons

Input voltage (V)	Load (KW)	Load voltage (V)			Load Current (A)			% THD of Load voltage		
		PI	SMC	Hardware	PI	SMC	Hardware	PI	SMC	Hardware
70	0.5	120	120	123	4.18	4.16	4.8	3.03	2.78	4.76
70	1.0	120	120	122	8.42	8.34	8.6	3.18	2.83	4.92
70	1.5	119.5	119.8	118	12.58	12.55	12.9	3.35	2.88	5.60
70	2.0	118.4	119.6	116	16.76	16.92	17.1	3.51	2.95	5.73
70	2.5	117.8	119.3	115	20.61	20.95	21.2	3.68	3.01	5.89

## VII. CONCLUSION

The solar boost inverter has been modelled from the basic principles and the SMC designed to govern its operation. The effort has been oriented to ensure the regulation of the output voltage of the inverter across the operating range and reject servo and regulatory disturbances. The scheme has been ordained to lower the THD of the output voltage in an attempt to increase the fundamental component of the load voltage. The simulation results have been portrayed to claim the supremacy for the SMC and allow a scope for the use of such inverter in real world applications. The validation through a prototype model has been ordained to further strengthen the claim of the merits of the use.

## REFERENCES

- [1]. Kalyan Chakravarthy Palagiri, Dasari Uma Maheswara Rao, "Grid Connected Current Controlled Boost Inverter Based Battery Supported Fuel cell", International Journal & Magazine of Engineering, Technology, Management and Research.
- [2]. Ravindranath Adda, *Student Member, IEEE*, Santana Mishra, *Member, IEEE*, and Avinash Joshi, "A PWM Control Strategy for Switched Boost Inverter" 978-1-4577-0541-0/11/\$26.00 ©2011 IEEE
- [3]. Guo-Rong Zhu, Cheng-Yuan Xiao, Hao-Ran Wang, Wei Chen, Siew-Chong Tan "Dynamic Characteristics of Boost Inverter with Waveform Control" IEEE
- [4]. Anusree V and Saifunnisa P, "Closed Loop Control of Switched Boost Inverter" International Conference on Electrical, Electronics, and Optimization Techniques (ICEEOT) - 2016
- [5]. Minsoo Jang, Takyun Kim and Vassilios G. Agelidis, "Design and Implementation of a 200 kHz Single-Phase Boost-Inverter Using Silicon Carbide Semiconductors" IECON2015-Yokohama November 9-12, 2015
- [6]. Minh-Khai Nguyen, *Member, IEEE*, and Tan-Tai Tran "Quasi Cascaded H-Bridge Five-Level Boost Inverter" DOI 10.1109/TIE.2017.2701770, IEEE

- [7]. Songwei Huang<sup>1</sup>, Fen Tang<sup>1,2</sup>, Zhen Xin<sup>3</sup>, Qi Xiao<sup>1</sup> and Poh Chiang Loh<sup>1</sup>, “High Performance Current Control Strategy for Grid-Connected Boost DC-AC Inverter” *IEEE Trans. Ind. Electron.*, 2017.
- [8]. Rong-Jongwai, Yao-Kailiu,” Design of Fuzzy Neural Network Control of single stage boost inverter” proceeding of 2015 International Conference of Machine learning and cybernetics, Guangzhou, July 2015.
- [9]. Minh-Khai Nguyen, *Member, IEEE*, and Tan-Tai Tran “A Single-Phase Single-Stage Switched-Boost Inverter with Four Switches” DOI 10.1109/TPEL.2017.2754547, *IEEE Transactions on Power Electronics*
- [10]. Ashraf Ali Khan, *Student Member, IEEE*, Honnyong Cha, *Member, IEEE*, Hafiz Furqan Ahmed, Juyong Kim, and Jintae Cho, “A Highly Reliable and High Efficiency Quasi Single-Stage Buck-Boost Inverter” DOI 10.1109/TPEL.2016.2598251, *IEEE Transactions on Power Electronics*
- [11]. Siew-Chong Tan, *Member, IEEE*, Y. M. Lai, *Member, IEEE*, and Chi K. Tse, *Fellow, IEEE* “A Unified Approach to the Design of PWM-Based Sliding-Mode Voltage Controllers for Basic DC-DC Converters in Continuous Conduction Mode” *IEEE TRANSACTIONS ON CIRCUITS AND SYSTEMS—I: REGULAR PAPERS*, VOL. 53, NO. 8
- [12]. M.T. Zhang, M. M. Jovanovic, F. C. Lee. “Analysis and Evaluation of Interleaving Techniques in Forward Converters” *IEEE Transactions on Power Electronics*, Volume 13, No.4.
- [13]. B. Mahesh Kumar<sup>1</sup>, S. M. Zafarullah<sup>2</sup>, “Boost Inverter Based Single Phase Grid Connected Fuel Cell System” *IJESC* vol. 19, no. 5,
- [14]. M.Kaliamoorthy, R.M.Sekar, I.Gerald Christopher Raj “Solar Powered Single Stage Boost Inverter with ANN Based MPPT Algorithm” *ICCCCT-10*, international conference on cement, concrete and construction technology.

S.Sivaranjani. “Design of a Sliding Mode Controller for a Solar Boost Inverter.” *.IOSR Journal of Engineering (IOSRJEN)*, vol. 08, no. 12, 2018, pp. 28-37.